

Magnetic field-induced exchange effects between Mn ions and free carriers in $ZnSe$ quantum well through the intermediate nonmagnetic barrier studied by photoluminescence

D. M. Zayachuk,¹ T. Slobodskyy,^{2,3,*} G. V. Astakhov,^{2,4} A. Slobodskyy,^{5,6}
C. Gould,² G. Schmidt,^{2,7} W. Ossau,² and L. W. Molenkamp²

¹*Lviv Polytechnic National University - 12 Bandera St, 79013 Lviv, Ukraine*

²*Physikalisches Institut der Universität Würzburg - 97074 Würzburg, Germany*

³*Present address: Institute for Synchrotron Radiation,*

Karlsruhe Institute of Technology - 76344 Eggenstein-Leopoldshafen, Germany

⁴*A. F. Physico-Technical Institute, Russian Academy of Sciences - 194021 St. Petersburg, Russia*

⁵*Light Technology Institute, Karlsruhe Institute of Technology (KIT), Kaiserstr. 12, 76131 Karlsruhe, Germany*

⁶*Zentrum für Sonnenenergie- und Wasserstoff-Forschung Baden-Württemberg, Industriestr. 6, 70565 Stuttgart, Germany*

⁷*Present and permanent address: Institut für Physik, Universität Halle - 06099 Halle, Germany*

(Dated: November 18, 2018)

Photoluminescence (PL) of the 50 nm $Zn_{0.9}Be_{0.05}Mn_{0.05}Se$ / d nm $Zn_{0.943}Be_{0.057}Se$ / 2.5 nm $ZnSe$ / 30 nm $Zn_{0.943}Be_{0.057}Se$ structures is investigated as a function of magnetic field (B) and thickness (d) of intermediate $Zn_{0.943}Be_{0.057}Se$ nonmagnetic barrier between the $Zn_{0.9}Be_{0.05}Mn_{0.05}Se$ semimagnetic barrier and $ZnSe$ quantum well at the temperature 1.2 K. The rate of the shift of different PL bands of the structures under study is estimated in low and high magnetic fields. The causes of the shift rate increase under pass from low to high magnetic fields are interpreted. The peculiarities of the effect of the intermediate barrier on the luminescence properties of the structures are presented. It is shown that deformation of adjacent layers by the barrier plays a crucial role in the formation of these properties, especially in forming the Mn complexes in the $Zn_{0.9}Be_{0.05}Mn_{0.05}Se$ layer. The change of the band gap as well as of the donor and acceptor levels energies under the effect of biaxial compression of the $Zn_{0.9}Be_{0.05}Mn_{0.05}Se$ layer by the $Zn_{0.943}Be_{0.057}Se$ are estimated. It is concluded that the $Zn_{0.943}Be_{0.057}Se$ intermediate barrier also appreciably changes the effect of giant Zeeman splitting of the semimagnetic $Zn_{0.9}Be_{0.05}Mn_{0.05}Se$ barrier energy levels on the movement of the energy levels of $ZnSe$ quantum well in a magnetic field and on polarization of the quantum well exciton emission.

I. INTRODUCTION

Quantum heterostructures containing layers of diluted magnetic semiconductors (DMS), usually a $3d$ Mn or Fe based transition metal, have been extensively studied in the literature. The main focus has been made on both fundamental and practical applications, especially these designed for different spin-electronic devices. Presence of transition element ions provides the conditions for magnetic tuning of the heterojunction band alignment due to extraordinarily large spin-splitting of the DMS bands due to the exchange interaction between the s and p band electrons and $3d^5$ electrons associated with the $3d$ element ions¹⁻³. The s , $p-d$ exchange interaction between the local moments and the band electrons gives rise to a rich spectrum of collective magnetic behavior. When an external magnetic field is applied to DMS, they exhibit two distinct band gaps, one for each spin direction¹. This splitting of conduction and valence bands (giant Zeeman splitting) can lead to a sizable spin polarization of the carriers in the DMS. This property is used to inject spin-polarized carriers into nonmagnetic semiconductors^{4,5}.

Two typical approaches are usually applied to the fabrication of DMS heterostructures: a heterostructure with a DMS layer as a quantum well (QW)⁶ or a heterostructure with DMS layers as quantum barriers^{7,8}. In the first case, both the free carriers and the $3d$ element ions

are located in the same layer of a QW. This leads to a strong interaction between the free carriers and the localized $3d$ -electrons of ions which intensifies the effects caused by the magnetic field. However, the presence of magnetic impurities in a quantum well stimulates spin relaxation processes⁹⁻¹¹. Hence, it is preferable to separate the carriers from the magnetic media¹²⁻¹⁴. In this case, the exchange interaction between the free $2D$ carriers of nonmagnetic quantum well and the ions of magnetic impurities in the barrier is driven by penetration of the carrier wave function tails into the barrier.

The effective depth of a well, represented by the difference between the positions of the band edges in adjacent layers, is strongly dependent on the magnetic field. At the same time, the energy of quantization levels in a shallow well strongly depends on the well depth. Therefore, the electron states in a nonmagnetic quantum well acquire some characteristics of the DMS materials, specifically sensitivity to the magnetic field¹.

It seems interesting to investigate the effect of magnetic field on the electron states in a nonmagnetic quantum well effected by a semimagnetic barrier. The barrier changes its height and exchange interaction with the states. Separation of the two effects can provide an additional degree of freedom in fabricating spintronics devices. In particular, an additional nonmagnetic layer introduced between a semimagnetic barrier and a

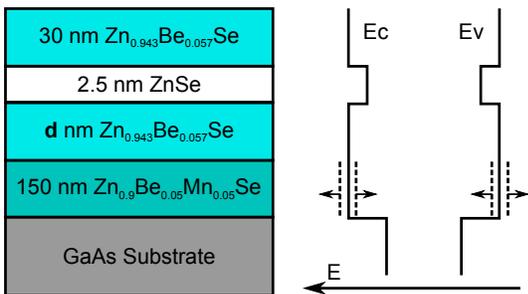


FIG. 1. Schematic view of the sample layout (left) with the corresponding energy band profile (right). The spin-split subbands of the conduction band (E_C) and the valence band (E_V) in the magnetic field are depicted by arrows. The $Zn_{0.943}Be_{0.057}Se$ barrier thickness d was varied as 0 (named $a1$), 2.5 ($b1$), 7.5 ($c1$), and 12.5 nm ($d1$).

nonmagnetic quantum well may be used for this purpose. Since, in the range of our experimental conditions, the nonmagnetic barrier height only negligibly depends on a magnetic field, the changes of an exchange interaction contribution will dominate in the field behavior of the energy characteristics of the QW. In this paper we show such a possibility using the example of quantum structures based on the $ZnSe$ quantum well with the $Zn_{0.9}Be_{0.05}Mn_{0.05}Se$ and $Zn_{0.943}Be_{0.057}Se$ barriers. The barrier compositions were selected based on the condition of an approximate parity of the band gap of the barriers at zero magnetic field. In order to study the field-induced exchange effects through the intermediate nonmagnetic barrier between Mn ions and free carriers in $ZnSe$ quantum well, $Zn_{0.943}Be_{0.057}Se$ barrier of different thickness was introduced between the $ZnSe$ and $Zn_{0.9}Be_{0.05}Mn_{0.05}Se$ layers. Photoluminescence (PL) properties of the structure in magnetic fields up to 5.25 T were investigated.

II. EXPERIMENTAL DETAILS

The samples used in the PL experiments were grown by molecular beam epitaxy on a $GaAs$ substrate. The sample layout is depicted in Fig. 1. The nonmagnetic space layer d is used for the purpose of varying the magnetic interaction in the structure.

PL spectra at 1.2 K in magnetic fields up to 5.25 T at Faraday geometry were measured to study the peculiarities of the exchange interaction between the Mn ions and free carriers. For optical excitation, we used a stilbene-3 dye laser pumped by ultraviolet lines of an Ar-ion laser. For non-resonant excitation, the laser energy is tuned to $E_{exc} = 2.94$ eV exceeding the band gap of the $Zn_{0.9}Be_{0.05}Mn_{0.05}Se$ barrier.

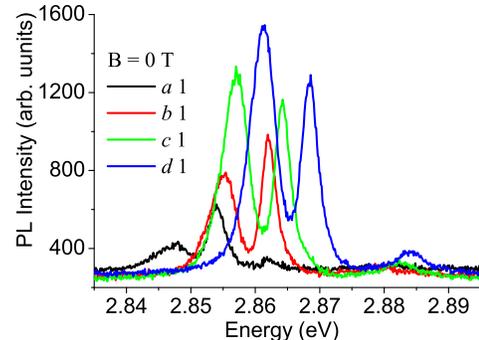


FIG. 2. The PL spectra of the 150 nm $Zn_{0.9}Be_{0.05}Mn_{0.05}Se$ / d nm $Zn_{0.943}Be_{0.057}Se$ / 2.5 nm $ZnSe$ / 30 nm $Zn_{0.943}Be_{0.057}Se$ structures in zero magnetic fields: $T = 1.2$ K. $\hbar\nu_{ex} = 2.94$ eV.

III. THE EXPERIMENTAL PL SPECTRA

Fig. 2 shows the PL spectra for the structures under study without the application of magnetic field. One can see that the shape of PL spectrum critically depends on the presence of an intermediate $Zn_{0.943}Be_{0.057}Se$ barrier between the $ZnSe$ QW and the semimagnetic $Zn_{0.9}Be_{0.05}Mn_{0.05}Se$ layer. This concerns the two "evident" spectra characteristics, i. e., the number of the PL bands and their intensity. The most striking feature of this dependence is a decrease of the number of PL bands by one for the structures with an intermediate barrier.

The composition of the structure also affects the behavior of the PL bands in the magnetic field where the bands split into two components with σ^+ and σ^- polarization. Fig. 3 shows this effect using the example of different polarization PL spectra in a magnetic field up to 1 T for $a1$ and $d1$ structures.

In order to quantitatively analyze the structure composition effect on the behavior of PL spectra in a magnetic field, it is necessary to separate the spectra into elementary components. This turns out to be very complicated problem, especially in the range of high magnetic fields where different PL bands superimpose one above another. As a result, the experimental PL spectrum can be reproduced in different ways by the same number of elementary bands. As an example, the data in Fig. 4 illustrate this.

In view of the mentioned ambiguity, decomposition of the experimental spectra into elementary constituents was carried out using the method of averaging. Details of the method of decomposition will be discussed more in detail elsewhere. Here we emphasize that it is well known¹² that for the zinc-blende structure, the transition matrix element of the transitions involving heavy holes (hh) is three times larger than that involving light holes (lh). Therefore, only those decompositions were taken into account where the PL intensity of the heavy

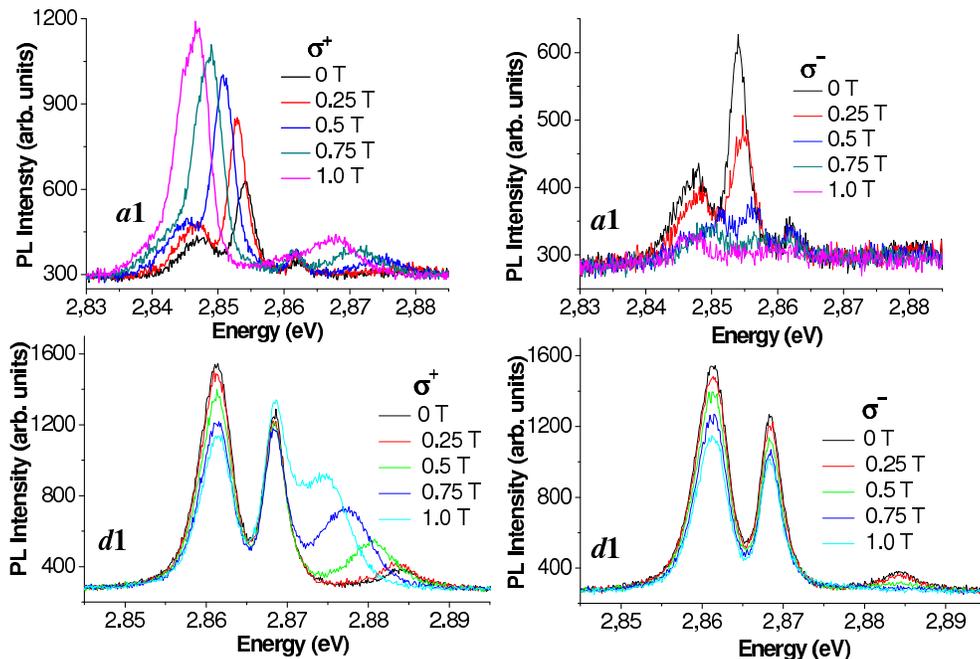


FIG. 3. The PL spectra of σ^+ and σ^- -polarization of the $a1$ (top) and $d1$ (bottom) structures in magnetic fields.

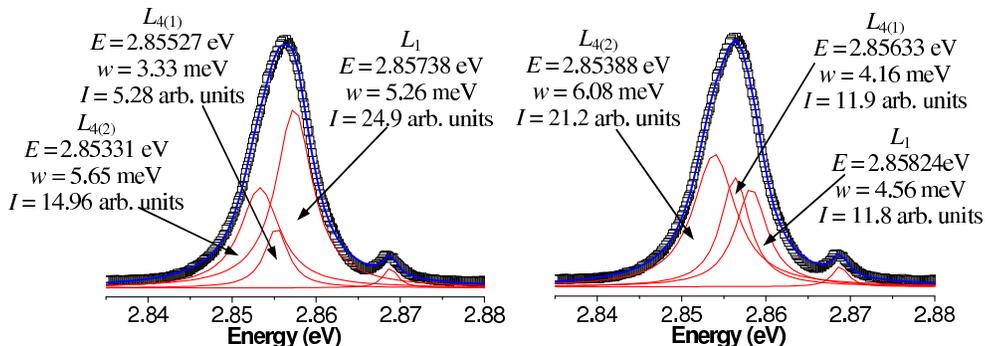


FIG. 4. Two examples of a multitude of decompositions of the experimental σ^+ -polarized PL spectrum of the $d1$ structure in 5 T magnetic fields on the Lorentz components satisfying a requirement of a domination of the intensity of the heavy excitons (the left band) over the intensity of the light excitons (the second band from the left) in the $ZnSe$ QW. Classification of the $L_1 - L_4$ bands see below in Sec. IV, their nature - in Sec. VIII.

excitons was larger than the PL intensity of the light excitons. It will be shown below that exactly these excitons form the longest wave PL bands of the structures under study. Not less than 20 different decompositions covering the maximum range of parameter variations for each spectrum were used to determine the averaged values of the parameters. An analysis showed that the deviation of experimental values of the parameters of different decompositions from their averaged values in any structures do not exceed: (i) ± 0.0005 eV for the energy of a short wave component of the spectra and ± 0.0015 eV for the long wave components; (ii) $\pm 20\%$ of the averaged value for the full width at half maximum (FWHM) of the bands; $\pm 60\%$ of the averaged value for the intensity of the bands. The total intensity of PL is reproduced by the

intensity of the Lorentz components within the error of no more than 10 % of the true value.

IV. ENERGY POSITION OF THE PL BANDS

Fig. 5 shows the magnetic field dependences on the energy positions of different PL bands for the structures under study. Let us examine these dependences from viewpoint of general and distinctive features in different structures.

The L_1 band: It is the highest energy PL band in zero magnetic fields. Its behavior in a magnetic field is the same for all structures. The σ^+ -polarized L_1^+ band shifts to the long-wave range, if B increases. The σ^- -polarized

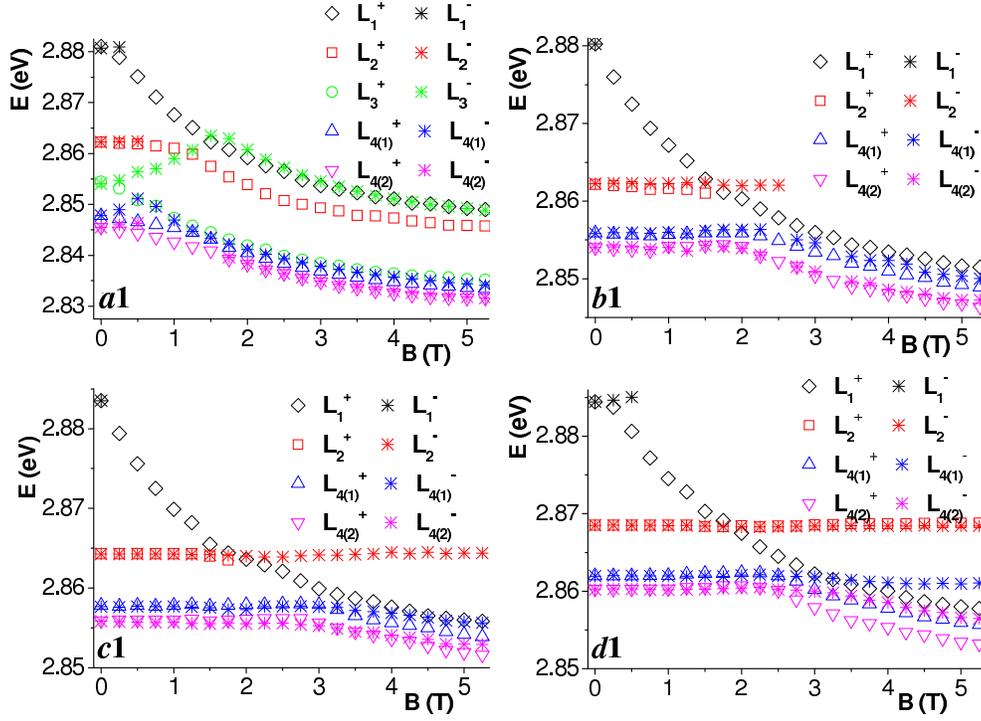


FIG. 5. Magnetic field dependence of the energy positions of the Lorentz components of both σ^+ ($L_1^+ - L_{4(2)}^+$) and σ^- -polarizations ($L_1^- - L_{4(2)}^-$).

L_1^- band tends to shift in the opposite direction in a magnetic field and practically disappears when $B > 0.5$ T.

The L_2 band: It is the next PL band in zero magnetic fields. It behaves differently in different structures. σ^+ -polarization: (i) the a1 structure: the L_2^+ band slightly changes its position in low (< 1 T) magnetic fields and shifts appreciably to the long-wave range in high magnetic fields, when B increases; (ii) the b1 and c1 structures: the L_2^+ band energy practically does not depend on the magnetic field for $B < 1.25$ T, then starts to decrease somewhat. The band disappears in the magnetic field where its energy becomes equal to the L_1^+ band energy; (iii) the d1 structure: the L_2^+ band position does not depend on the magnetic field. σ^- -polarization: the L_2^- band energy does not depend on the magnetic field. However, the range of magnetic fields where the band is observed is different for different structures. It is the narrowest ($B \leq 0.5$ T) for the a1 structure and includes all magnetic fields under investigation for the c1 and d1 structures.

The L_3 band: This band displays the strongest dependence on the structure composition. It is observed only for the a1 structure without the intermediate $Zn_{0.943}Be_{0.057}Se$ barrier. The L_3^+ band energy decreases if B increases. On the contrary, in low magnetic fields of approximately $B < 1.5$ T, the L_3^- band energy increases if B increases. If $B > 1.5$ T, the L_3^- band shifts in the opposite direction. In the fields above 2 T its energy position coincides with the energy position of the L_1^+ band.

The L_4 band: This is the smallest energy PL band in zero magnetic fields. This band is a superposition of two components with close energy. We mark them $L_{4(1)}^+$, $L_{4(2)}^+$ and $L_{4(1)}^-$, $L_{4(2)}^-$ for σ^+ and σ^- -polarization, respectively. Their behavior is absolutely different for the structures with and without an intermediate nonmagnetic $Zn_{0.943}Be_{0.057}Se$ barrier. *The a1 structure:* (i) the energy position of the L_4 bands changes if B changes within the whole range of magnetic field under study; (ii) the $L_{4(1)}^+$ and $L_{4(2)}^+$ bands shift to the long-wave range if B increases; (iii) if the magnetic field is applied, the $L_{4(1)}^-$ and $L_{4(2)}^-$ bands shift to the short-wave range but they change the direction of their shift if $B > 0.5$ T. In this range they follow the positions of the respective PL bands of σ^+ -polarization. *The b1, c1, and d1 structures:* (i) in low magnetic field, the energy of the bands practically does not depend on the magnetic field and thus the $L_{4(1)}^+$ and $L_{4(1)}^-$ as well as $L_{4(2)}^+$ and $L_{4(2)}^-$ coincide with each other; (ii) in high magnetic field, all bands shift to the long-wave range and the bands with different polarizations gradually diverge. The thicker is the intermediate barrier the larger is the divergence of both L_4^+ and L_4^- bands.

V. FULL WIDTH AT HALF MAXIMUM OF THE PL BANDS

Fig. 6 and Fig. 7 show the effect of both the intermediate barrier and the magnetic field on the PL bands FWHM w for the structures under study.

The main features of this effect are as follows.

The L_1 band: FWHM of the L_1^+ band is the widest in the $a1$ structure. In zero magnetic fields, ω decreases if the intermediate nonmagnetic barrier is applied and its thickness increases. In low magnetic field $B < 1$ T, the band behavior is different for different structures: from continuous decrease in the $a1$ structure to some increase in the $d1$ structure if B increases. For $B > 1$ T, w monotonously decreases if B increases. Herein the band is practically of the same width in all structures with the intermediate $Zn_{0.943}Be_{0.057}Se$ nonmagnetic barrier.

The L_2 band: FWHM of the L_2^+ band increases approximately three times under transition from low to high magnetic fields for the $a1$ structure and somewhat decreases for the $d1$ structure. FWHM of the L_2^- band practically does not depend on B for the $c1$ and $d1$ structures where it is observed for any investigated magnetic fields.

The L_3 band: If a magnetic field is applied, FWHM of the L_3^+ band somewhat decreases and that of the L_3^- band increases. After changing the shift direction in a magnetic field, the L_3^- band FWHM decreases if B increases. In this range of the magnetic field it is approximately four times larger than the L_3^+ band FWHM.

The L_4 band: FWHM of the $L_{4(1)}^+$ and $L_{4(2)}^+$ bands practically does not depend on B in low magnetic fields $B < 1$ T and decreases if the intermediate nonmagnetic barrier is applied and its thickness increases. In the intermediate magnetic fields, $w(L_{4(2)}^+)$ and $w(L_{4(1)}^+)$ sharply rise in the structures with an intermediate barrier. The band widening depends on the barrier thickness d : it is the largest for the $b1$ structure where d is the smallest and vice versa - it is the smallest for the $d1$ structure where d is the largest. If B increases further, $w(L_{4(2)}^+)$ and $w(L_{4(1)}^+)$ starts to decrease. The FWHM decrease slackens if the barrier thickness increases. For the $d1$ structure, $w(L_{4(2)}^+)$ and $w(L_{4(1)}^+)$ practically do not depend on B in the high magnetic field range. In this range of the field for the $a1$ structure, $w(L_{4(2)}^+)$ and $w(L_{4(1)}^+)$ somewhat increase if B increases.

FWHM of both $L_{4(1)}^-$ and $L_{4(2)}^-$ bands behaves like to $L_{4(1)}^+$ and $L_{4(2)}^+$ bands FWHM.

VI. INTENSITY OF THE PL BANDS

Fig. 8 and 9 show an effect of both the intermediate barrier and magnetic field on the PL band intensity I for the structures under study.

The application of the intermediate nonmagnetic

barrier $Zn_{0.943}Be_{0.057}Se$ between the $ZnSe$ and $Zn_{0.9}Be_{0.05}Mn_{0.05}Se$ layers of the structure has no effect on the L_1 band intensity in zero magnetic fields but appreciably augments the intensity of the other PL bands - L_2 , QW ($I(L_{4(1)})+I(L_{4(2)})$) as well as the total PL intensity. All these intensities increase if $d(Zn_{0.943}Be_{0.057}Se)$ increases (Fig. 8).

Application of a magnetic field increases the intensity of the short wave L_1^+ PL band in any structures. At the same time, the field effect on the behavior of the other PL bands is not that simple. For example, in a low magnetic field $B < 1$ T, an intensity of the long wave $L_{4(1)}^+$ and $L_{4(2)}^+$ bands increase when B increases in the $a1$ structure but decreases in another three structures. An intensity of the L_2^+ band increases under transition from low to high magnetic fields in the $a1$ structure but decreases and comes off plateau in the $d1$ structure (Fig. 9).

Application of a magnetic field also increases the total intensity $I_{\sigma+}$ of the σ^+ -polarized emission of the structures but decreases the total intensity $I_{\sigma-}$ of the σ^- -polarized emission (Fig. 10). In high magnetic fields, $I_{\sigma-}$ first stabilizes and then displays a weak tendency to increase. Herein $I_{\sigma-}$ becomes much smaller than $I_{\sigma+}$. For the top magnetic field, $B = 5.25$ T ratio $I_{\sigma+}/I_{\sigma-}$ changes from 0.04 in the $a1$ structure to 0.14 for the $d1$ structure (see inset in Fig. 10, (b)).

In low magnetic fields, the character of $I_{\sigma+}(B)$ appreciably depends on the intermediate barrier thickness: the thicker is the barrier the weaker is the dependence. In high magnetic fields, an effect of the intermediate barrier thickness on the total intensity $I_{\sigma+}$ of the structures has got a pronounced non-monotonous character. The thinnest barrier (the $b1$ structure) does not increase $I_{\sigma+}$ with respect to the $a1$ structure. Similar increase of the intermediate barrier thickness from 7.5 to 12.5 nm (the $c1$ and $d1$ structures) practically does not change the parameter $I_{\sigma+}$ as well. Thus it is possible to reach the principal increase of the total PL intensity $I_{\sigma+}$ in the high magnetic fields by changing the intermediate barrier thickness within the limits of 2.5 - 7.5 nm. The application of the intermediate barrier also appreciably affects the relative increase of $I_{\sigma+}(B)$ enfeebling it. Herein the barrier thickness is of minor importance (see inset in Fig. 10, (a)).

VII. POLARIZATION OF THE PL BANDS

Polarization of the PL bands is traditionally determined as $\rho = (I_{\sigma+} - I_{\sigma-})/(I_{\sigma+} + I_{\sigma-})$. The shortest L_1^- PL band disappears as early as $B > 0.5$ T in any structure under study. Thus, the intermediate barrier does not effect polarization of the L_1 band, which arises as soon as a magnetic field is applied and reaches 100 % if $B > 0.5$ T. The state of matter is absolutely different for the longest L_4 PL band. Fig. 11 demonstrates it by the example of the $L_{4(2)}$ bands.

As one can see, the $L_{4(2)}$ band is not polarized up to

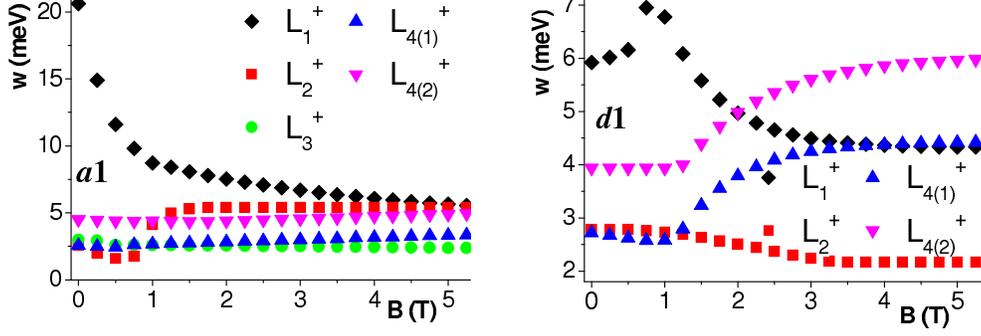


FIG. 6. Magnetic field dependence of the FWHM of the σ^+ -polarized bands of the *a1* and *d1* structures.

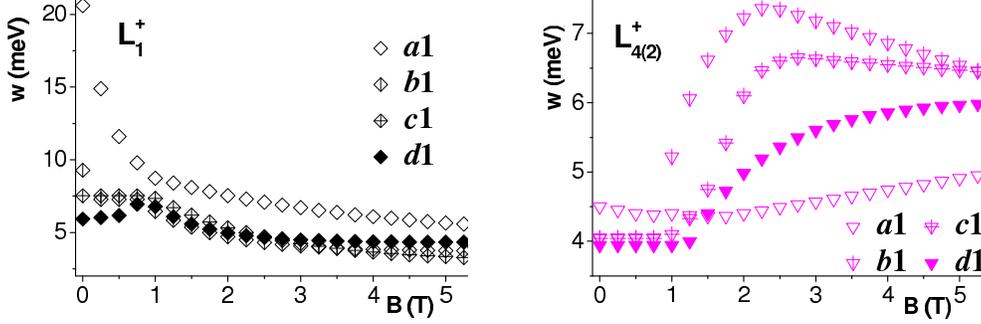


FIG. 7. Magnetic field dependence of the FWHM of the L_1^+ and $L_{4(2)}^+$ bands for all structures.

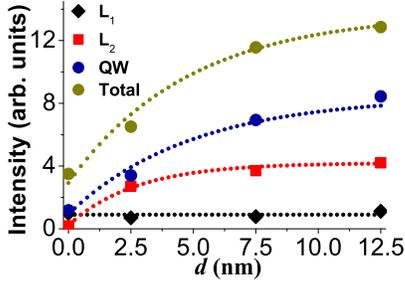


FIG. 8. Barrier thickness $d(\text{Zn}_{0.943}\text{Be}_{0.057}\text{Se})$ dependence of PL signal intensity at zero magnetic field.

$B \approx 1$ T for the *c1* and *d1* structures. At the same time, for the other two structures with the thinnest intermediate barrier and without a barrier the $L_{4(2)}$ band starts to polarize as soon as a magnetic field is applied. In the high magnetic fields, the $L_{4(2)}$ band polarization saturates. The polarization of saturation is the largest in the *a1* structure without any intermediate barrier (91 %), somewhat smaller for the *b1* and *c1* structures (89 - 88 %), and noticeably smaller for the *d1* structure with the thickest intermediate barrier (71 %). The polarization of the $L_{4(1)}$ band is the same.

VIII. DISCUSSION

In our previous work¹³ we analyzed the PL spectra of the *a1* structure and proposed the following interpretation of the origin of different bands. *Low magnetic fields*: (i) a transition between the $\text{Zn}_{0.9}\text{Be}_{0.05}\text{Mn}_{0.05}\text{Se}$ conduction band E_{ZnBeMnSe}^C and the energy level of an acceptor complex containing *Mn* E_{ZnBeMnSe}^{Mn} forms the short wave L_1 band; (ii) a donor-acceptor transition $E_{\text{ZnBeMnSe}}^D - E_{\text{ZnBeMnSe}}^A$ in $\text{Zn}_{0.9}\text{Be}_{0.05}\text{Mn}_{0.05}\text{Se}$ forms the L_2 band; (iii) an indirect transition in real space between the 2D conduction band of the *ZnSe* QW E_{ZnSe}^C and E_{ZnBeMnSe}^{Mn} forms the L_3 band. *High magnetic fields*: (i) a transition between E_{ZnBeMnSe}^C and the barrier valence band E_{ZnBeMnSe}^V forms the L_1 band; (ii) a transition $E_{\text{ZnBeMnSe}}^D - E_{\text{ZnBeMnSe}}^V$ forms the L_2 band; (iii) an indirect transition $E_{\text{ZnSe}}^C - E_{\text{ZnBeMnSe}}^V$ forms the L_3 band. The transitions within the *ZnSe* QW $E_{\text{ZnSe}}^C - E_{\text{ZnSe}}^V$ forms the L_4 band in any magnetic field. The short wave component $L_{4(1)}$ of the L_4 band is formed by emission of the light exciton, while the long wave component $L_{4(2)}$ is formed by emission of the heavy exciton. There are no reasons to expect that the intermediate $\text{Zn}_{0.943}\text{Be}_{0.057}\text{Se}$ barrier changes the nature of the PL bands within both the *ZnSe* QW and the $\text{Zn}_{0.9}\text{Be}_{0.05}\text{Mn}_{0.05}\text{Se}$ semimagnetic barrier. Therefore, the analysis that follows the origin of the L_1 , L_2 , and L_4 bands is the same as in the other three structures.

In order to separate the contribution of the barrier

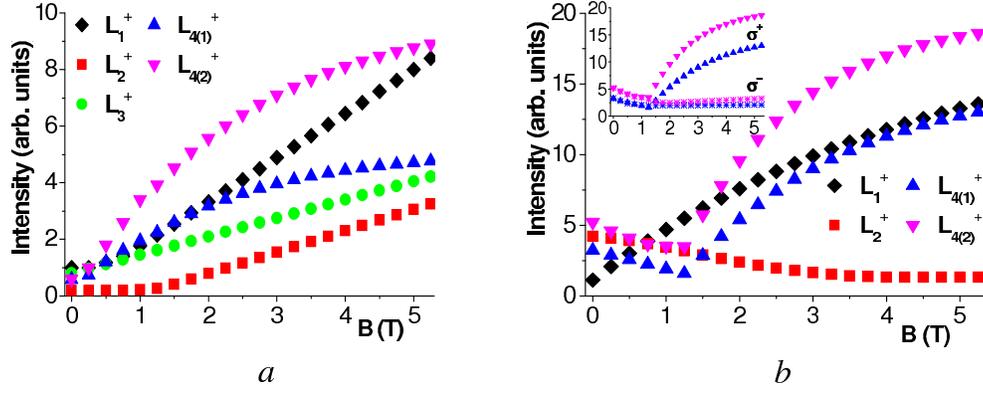


FIG. 9. Magnetic field dependence of the PL intensity of the σ^+ - polarized bands for both *a1* (left) and *d1* (right) structures. Inset: PL intensity of both $L_{4(1)}$ and $L_{4(2)}$ bands of σ^+ and σ^- polarization.

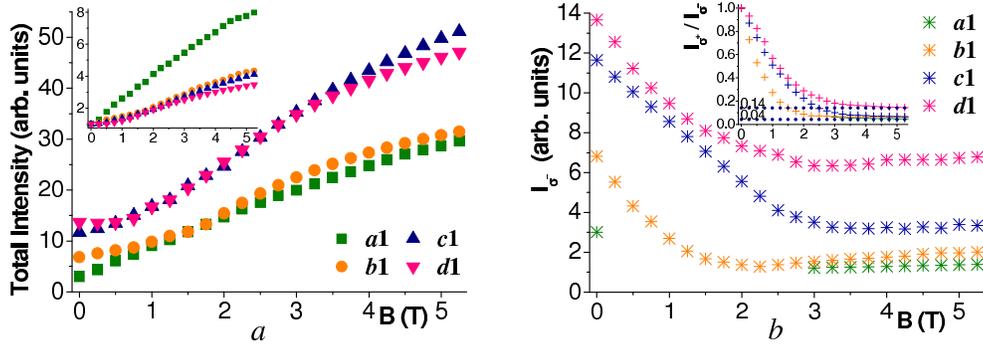


FIG. 10. Magnetic field dependence of a total intensity of σ^+ (left) and σ^- -polarized (right) PL of the structures under study. Insets: (left) - a total intensity normalized by its value in zero magnetic fields; (right) - a relation between a total intensity of σ^+ and σ^- -polarized PL.

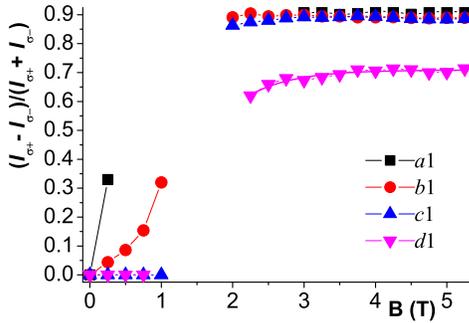


FIG. 11. Magnetic field dependence of the $L_{4(2)}$ band polarization.

height and exchange interaction in the field behavior of different PL bands, a quantitative analysis is needed.

The L_1 band shift in a magnetic field is caused by the giant Zeeman splitting and may be written as^{1,15,16}:

$$E(B) = E(0) \mp (\chi N_0) \tilde{x} \langle S_Z \rangle \quad (1)$$

$$\chi N_0 = \alpha N_0 - \beta N_0 \quad (2)$$

where \tilde{x} is the effective Mn concentration, αN_0 and βN_0 are the exchange integrals between the Mn ions and carriers for upper and lower states responsible for this PL band, respectively, $\langle S_Z \rangle$ is the thermal average of the Mn spin given by:

$$\langle S_Z \rangle = \frac{5}{2} B_{5/2} [5\mu_B B / k_B(T + T_{eff})] \quad (3)$$

$B_{5/2}$ is Brillouin function of the argument in square brackets, μ_B is the Bohr magneton, k_B is the Boltzmann constant, T is the temperature, and T_{eff} is an empirical parameter representing antiferromagnetic interaction between the Mn ions. In our calculations, the parameter T_{eff} was taken to be equal to 1.75 K in accordance with the empirical ratio obtained in¹⁵ for $Zn_{1-x}Mn_xSe$.

A comparison of the experimental and the calculated data for all structures under study is presented in Fig. 12. It clearly shows that there are two ranges of magnetic fields for any structure where the rates of the L_1^+ band

shift (χN_0) in the $Zn_{0.9}Be_{0.05}Mn_{0.05}Se$ layer are different: they are smaller for low and larger for high magnetic fields. We marked them by $(\chi N_0)_{1L}$ and $(\chi N_0)_{1H}$, respectively. The parameter $E(0)$ is also different for the ranges of low and high magnetic fields. We marked them $E_{1L}(0)$ and $E_{1H}(0)$, respectively.

One can see in Fig. 12 that many of the parameters of the L_1 band in the $Zn_{0.9}Be_{0.05}Mn_{0.05}Se$ layer are different not only for low and high magnetic fields. They are also different for the structures with and without the intermediate $Zn_{0.943}Be_{0.057}Se$ barrier as well as for the structures of different barrier thickness. Let us examine these parameters.

$E_{1H}(0)$ has a sense of a band gap of the semimagnetic $Zn_{0.9}Be_{0.05}Mn_{0.05}Se$ barrier in zero magnetic fields. This parameter increases monotonously from 2.8932 eV for the barrier in the $a1$ structure to 2.9019 eV for the same barrier in the $d1$ structure (Fig. 12). We explain the observed changes of the parameters $E_{1H}(0)$ as well as of the energy of L_1 bands by both: (i) the effect of the strains of the $Zn_{0.9}Be_{0.05}Mn_{0.05}Se$ barrier surface layers caused by the action of the adjacent $ZnSe$ or $Zn_{0.943}Be_{0.057}Se$ layers on the band gap value; (ii) the dominant contribution of the strained surface layers in forming the emission bands of the semimagnetic barrier. It is well known that in the absence of strain, the maxima of the heavy- and light-hole valence bands are degenerate in the zinc-blende semiconductors. The biaxial strain shifts and splits the heavy- and light-hole bands. If the strain is compressive, the band gap increases and coincides with the heavy-hole-derived band gap. In the case of biaxial tension, the band gap shrinks and is associated with the light-hole transition¹⁷. The layers of the structures under study have different lattice constants: $a(ZnSe) = 5.6684 \text{ \AA}$, $a(Zn_{0.943}Be_{0.057}Se) = 5.6382 \text{ \AA}$, $a(Zn_{0.9}Be_{0.05}Mn_{0.05}Se) = 5.6592 \text{ \AA}$ ^{18,19}. Therefore, they deform each other: $ZnSe$ tenses the surface layers of $Zn_{0.9}Be_{0.05}Mn_{0.05}Se$, and $Zn_{0.943}Be_{0.057}Se$ compresses them. Thus, the $Zn_{0.9}Be_{0.05}Mn_{0.05}Se$ surface layers that contact with the $ZnSe$ layer, have a smaller band gap, and contacting with the $Zn_{0.943}Be_{0.057}Se$ layer have a larger band gap than the strainless one. It enables us to construct a dependence of the band gap of the strain $Zn_{0.9}Be_{0.05}Mn_{0.05}Se$ layers on the thickness of both the contact $ZnSe$ and $Zn_{0.943}Be_{0.057}Se$ layers which cause these strains. This dependence is presented in Fig. 13.

Fig. 13 shows that the band gap of the $Zn_{0.9}Be_{0.05}Mn_{0.05}Se$ strain layers asymptotically approaches the value 2.9043 eV under compression by the $Zn_{0.943}Be_{0.057}Se$ layer when $d(Zn_{0.943}Be_{0.057}Se)$ approaches 30 nm. Extrapolation of the data in Fig. 13 also shows that the band gap of the strainless $Zn_{0.9}Be_{0.05}Mn_{0.05}Se$ is equal to 2.894 eV. Thus, the biaxial strain of the $Zn_{0.9}Be_{0.05}Mn_{0.05}Se$ layer by the $Zn_{0.943}Be_{0.057}Se$ layer can increase the band gap of the former by approximately 10 meV.

The obtained dependences of $E(L_1^+)$ from B may be explained by the dependence of the band gap of

$Zn_{0.9}Be_{0.05}Mn_{0.05}Se$ on the strains if the strained contact layers provide the main contribution to the emission transitions. Note that the importance of the strained heterointerface for localization of excitons was already emphasized in initial investigations of the II-VI strained-layer heterostructures²⁰.

The value $E_{1H}(0) - E_{1L}(0)$ has a sense of an acceptor level depth of the Mn complex in the $Zn_{0.9}Be_{0.05}Mn_{0.05}Se$ strained surface layers. It is approximately one and a half times smaller in the compressed layers in comparison with the tensed one: 10 meV for the $Zn_{0.9}Be_{0.05}Mn_{0.05}Se$ barrier in the $a1$ structure against (15.5 ± 1.2) meV for the other three structures.

The values of $(\chi N_0)_{1H}$ and $(\chi N_0)_{1L}$ are determined by the exchange interaction splitting the electronic band and impurity levels. It is obvious from Fig. 12 that the $(\chi N_0)_{1H}$ values are the same for all structures. It means that the αN_0 and βN_0 exchange integrals for C and V bands of $Zn_{0.9}Be_{0.05}Mn_{0.05}Se$ layer develop with no effect of the 2D free carriers of the $ZnSe$ QW. On the contrary, the $(\chi N_0)_{1L}$ value is the same only for the structures with the intermediate $Zn_{0.943}Be_{0.057}Se$ barrier. For the $a1$ structure without any intermediate barrier it is larger by approximately 22 %. It means that the exchange integral for electronic states of the Mn complex in the structures under study develops appreciably with participation of the 2D free carriers of the $ZnSe$ QW. In accordance with our previous analysis¹³ the band exchange integrals for the $Zn_{0.9}Be_{0.05}Mn_{0.05}Se$ layer are equal to $\alpha N_0 = 0.104$ eV, $\beta N_0 = -0.264$ eV. The value of the exchange integral for electronic states of the Mn complex in the $a1$ structure is equal to 0.156 eV. Using the obtained $(\chi N_0)_{1L}$ value for the $b1$, $c1$, and $d1$ structures we see that the application of intermediate $Zn_{0.943}Be_{0.057}Se$ barrier decreases this value to 0.112 eV, i.e., by approximately 40 %.

We explain these results in the following way. There are two types of free carriers contributing to the exchange interaction in the strained surface layers of the $Zn_{0.9}Be_{0.05}Mn_{0.05}Se$ barrier: 3D carriers of the $Zn_{0.9}Be_{0.05}Mn_{0.05}Se$ barrier and 2D carriers of the $ZnSe$ QW. The wave functions of 3D carriers are quite extended and span a large number of lattice sites of the $Zn_{0.9}Be_{0.05}Mn_{0.05}Se$ barrier. On the contrary, only the tails of the wave functions of 2D carriers penetrate from QW into the barrier. This penetration decreases or is absent when the intermediate $Zn_{0.943}Be_{0.057}Se$ barrier appears between the $ZnSe$ and $Zn_{0.9}Be_{0.05}Mn_{0.05}Se$ layers. Thus, we can unambiguously conclude that 2D carriers of the $ZnSe$ QW give negligible contribution to the formation of exchange integrals for C and V bands of the $Zn_{0.9}Be_{0.05}Mn_{0.05}Se$ strained contact layers but their contribution to the exchange interaction between the Mn complexes in these layers is can be described by mixing of the $3d^5$ levels of Manganese with the states of 2D free carriers of the $ZnSe$ QW. This is possible only if the Mn complex concentration in the strained layers is larger than the concentration of Mn in the sites of crystal

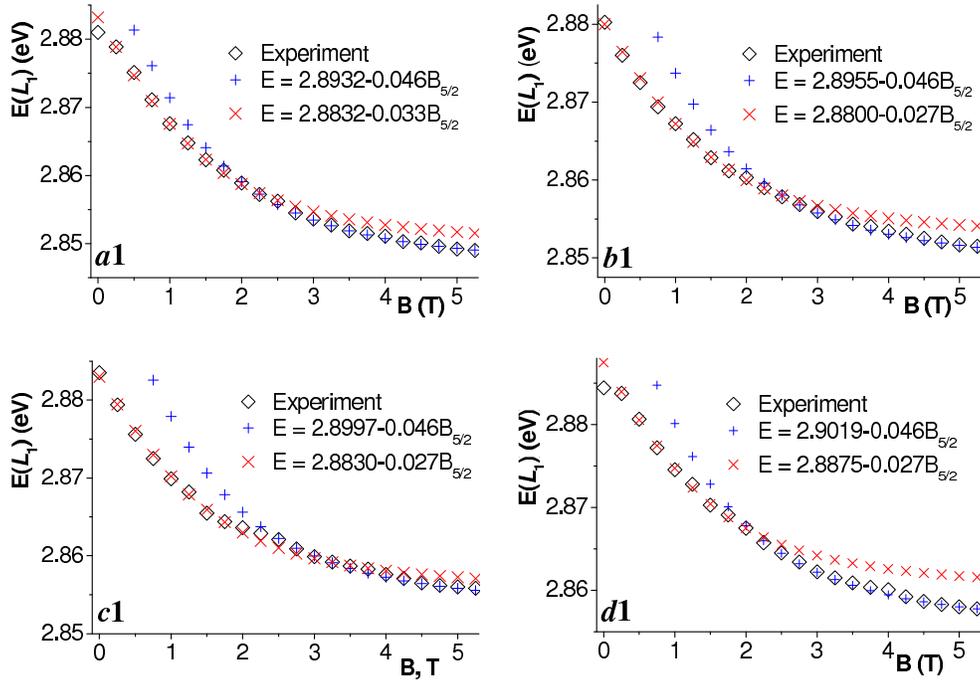


FIG. 12. Magnetic field dependence of the $E(L_1)$ for the different structures under study.

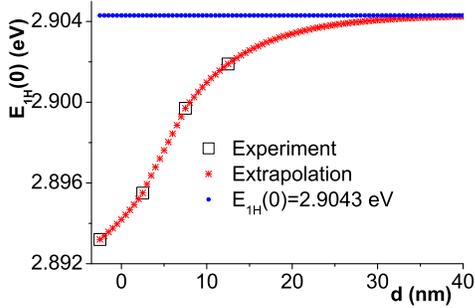


FIG. 13. $E_{1H}(0)$ vs d of the layers contacting with the $Zn_{0.9}Be_{0.05}Mn_{0.05}Se$ semimagnetic barrier in the investigated structures. d is positive for the $Zn_{0.943}Be_{0.057}Se$ layers (compression of $Zn_{0.9}Be_{0.05}Mn_{0.05}Se$ layer) and negative for $ZnSe$ layer (tension of $Zn_{0.9}Be_{0.05}Mn_{0.05}Se$ layer).

lattice. In other words, most probably the Mn complexes in $Zn_{0.9}Be_{0.05}Mn_{0.05}Se$ develop into the strained layers of a heterocontact.

Let us now consider the long wave L_4 PL band. The layer of the $ZnSe$ QW experiences compression on the part of both $Zn_{0.9}Be_{0.05}Mn_{0.05}Se$ and $Zn_{0.943}Be_{0.057}Se$ layers. As a result, its heavy- and light-hole bands split and the heavy-hole band defines the band gap in any structures under study. Therefore, the heavy excitons $|\pm 1\rangle = |\mp 1/2, \pm 3/2\rangle$ form the long wave component $L_{4(2)}^\pm$ of σ^+ and σ^- -polarization, respectively, and the light excitons $|\pm 1\rangle = |\pm 1/2, \pm 1/2\rangle$ form the short wave compo-

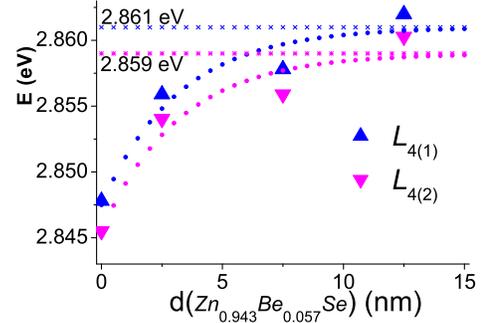


FIG. 14. Energy of the $L_{4(1)}^\pm$ and $L_{4(2)}^\pm$ bands vs. the intermediate $Zn_{0.943}Be_{0.057}Se$ barrier thickness in zero magnetic fields and their approximations.

nent $L_{4(1)}^\pm$ of the L_4 band.

A splitting between the energy of heavy and light excitons in zero magnetic fields is equal to (2.0 ± 0.3) meV for all structures. At the same time, the energies of both heavy and light excitons are different for different structures and increase with an increased thickness of the intermediate nonmagnetic barrier $Zn_{0.943}Be_{0.057}Se$ between the $Zn_{0.9}Be_{0.05}Mn_{0.05}Se$ and $ZnSe$ layers. The dependences of $E(L_{4(1)}^\pm)$ and $E(L_{4(2)}^\pm)$ on the thickness of the intermediate barrier in case of the absence of magnetic field are shown in Fig. 14.

One can see that both $E(L_{4(1)}^\pm)$ and $E(L_{4(2)}^\pm)$ increase if $d(Zn_{0.943}Be_{0.057}Se)$ increases and asymptotically ap-

proach the energy 2.861 and 2.859 eV, respectively. The cause of these changes is the same as in the case of the L_1 bands: the deformation effects. There is the following ratio between the lattice constants of the layers of the structures: $a(\text{ZnSe}) > a(\text{Zn}_{0.9}\text{Be}_{0.05}\text{Mn}_{0.05}\text{Se}) > a(\text{Zn}_{0.943}\text{Be}_{0.057}\text{Se})$. As a result, the $\text{Zn}_{0.943}\text{Be}_{0.057}\text{Se}$ layer more strongly compresses the ZnSe QW layer than the $\text{Zn}_{0.9}\text{Be}_{0.05}\text{Mn}_{0.05}\text{Se}$ layer and its deformation effect increases if $d(\text{Zn}_{0.943}\text{Be}_{0.057}\text{Se})$ increases. Therefore, the ZnSe layer band gap increases and the exciton energy increases too. For the $a1$ structure in zero magnetic fields $E(L_{4(1)}^{\pm}) = 2.8478$, and $E(L_{4(2)}^{\pm}) = 2.8455$ eV. It is seen that under the effect of the intermediate barrier, the heavy-hole-derived band gap of the ZnSe QW increases by 13 meV extra.

Application of a magnetic field splits the band edges in the well. However, the Zeeman splitting for nonmagnetic ZnSe should be negligible taking into account the g-factor value for electrons and holes²¹. Actually $E(L_{4(1)}^{\pm})$ and $E(L_{4(2)}^{\pm})$ negligibly depends on B only for the $b1$, $c1$, and $d1$ structures and only in magnetic fields $B < (2.0 \div 2.5)$ T (Fig. 5). For higher magnetic fields, the energy of L_4 exciton bands appreciably decreases. There are more essential changes in the energy positions of both $L_{4(1)}^{\pm}$ and $L_{4(2)}^{\pm}$ bands in a magnetic field for the $a1$ structure, as we have emphasized above. It is obvious that the exchange interaction between free carriers of the QW and Mn ions of the semimagnetic barrier, which is further modified by the intermediate nonmagnetic barrier, causes the observed changes.

The $a1$ structure is the structure with a shallow nonmagnetic QW having the adjacent layer of semimagnetic semiconductor. Therefore, the effective depth of the well, given by the difference between the positions of the band edges in the adjacent layers, is strongly dependent on the magnetic field, and in a shallow well the energy of the size quantization levels is strongly dependent on the well depth. For the other structures, the situation is radically different. Herein the positions of the band edges of the $\text{Zn}_{0.943}\text{Be}_{0.057}\text{Se}$ layers adjacent to the QW negligibly depend on B and the height of the intermediate barrier also negligibly depends on B . At the same time, an effective barrier height for electrons and holes appreciably depends on B because the position of the band edges of the $\text{Zn}_{0.9}\text{Be}_{0.05}\text{Mn}_{0.05}\text{Se}$ layer depends on B . It changes a range of penetration of the wave functions of the ZnSe QW well free carriers in the barrier ($\text{Zn}_{0.9}\text{Be}_{0.05}\text{Mn}_{0.05}\text{Se} + \text{Zn}_{0.943}\text{Be}_{0.057}\text{Se}$) because the boundary conditions on the QW edge ($\text{Zn}_{0.943}\text{Be}_{0.057}\text{Se} / \text{ZnSe}$) change. However, a change of the height of the intermediate and effective barriers has got a different effect on the shift of both $L_{4(1)}^{\pm}$ and $L_{4(2)}^{\pm}$ bands. As soon as an intermediate barrier height changes, the L_4 band position also changes. In case of an effective barrier, the situation is different. As it follows from the obtained data, the E_{ZnBeMnSe}^{V+} edge should go down appreciably lower than

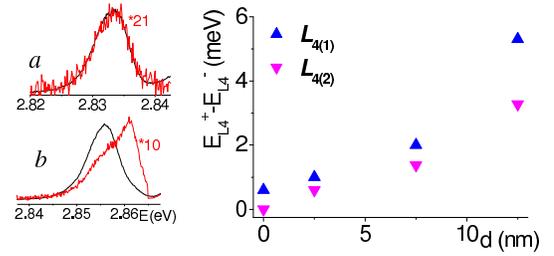


FIG. 15. The experimental PL spectra of the $a1$ (a) and $d1$ structures (b) of σ^+ (black lines) and σ^- -polarization (red lines) for $B = 5.25$ T in the energy range of the L_4 bands. Right - the shift between the energy positions of L_4^+ and L_4^- bands vs. $d(\text{Zn}_{0.943}\text{Be}_{0.057}\text{Se})$ at 5.25 T.

the E_{ZnSe}^{V+} edge before the L_4 bands change their position. In accordance with the energy diagram of the $a1$ structure¹³, the offset between the C and V bands of the $\text{Zn}_{0.9}\text{Be}_{0.05}\text{Mn}_{0.05}\text{Se}$ and $2D$ ZnSe layers distributed as $\Delta E_C / \Delta E_V = 60/40$ which is typical of these materials⁷. The intermediate barrier somewhat decreases the value $(E_{1H}(0) - E_{L_{4(2)}}(0))$, which determines the mutual location of the $\text{Zn}_{0.9}\text{Be}_{0.05}\text{Mn}_{0.05}\text{Se}$ and $2D$ ZnSe layer band edges on the energy scale. Its magnitude for the $a1$ structure is equal to 47.7 meV, and the averaged magnitude for the other three structures is equal to (42.3 ± 1.5) meV. If we share this value in proportion $\Delta E_C / \Delta E_V = 60 : 40$ we find that $E_{\text{ZnSe}}^{V+} - E_{\text{ZnBeMnSe}}^{V+}$ in zero magnetic field for the $b1$, $c1$, and $d1$ structures is equal to 16.9 meV. The energy of $L_{4(1)}^{\pm}$ and $L_{4(2)}^{\pm}$ bands start to decrease only if the E_{ZnBeMnSe}^{V+} goes down to approximately 24.5 meV ($B \approx 2$ T). However, one needs to remember that the effective barrier for both electrons and holes forming the L_4^+ bands goes down when B increases. On the contrary, the effective barrier for electrons and holes forming the L_4^- bands goes up. At the same time, the energy of $L_{4(1)}^{\pm}$ and $L_{4(2)}^{\pm}$ pair decreases in the range of high magnetic fields. It entirely bears a resemblance to the behavior of both $L_{4(1)}^{\pm}$ and $L_{4(2)}^{\pm}$ bands in the $a1$ structure in this magnetic range. In our previous work¹³ we explained such a behavior of different polarized exciton bands in the QW by the influence of the spin-flip processes caused by the degeneration of energy levels of the ZnSe QW and the $\text{Zn}_{0.9}\text{Be}_{0.05}\text{Mn}_{0.05}\text{Se}$ layer. We believe that the same processes also occur in the structures with the intermediate nonmagnetic barrier but the barrier presence somewhat changes the situation. The barrier weakens the interaction between the ZnSe QW and the $\text{Zn}_{0.9}\text{Be}_{0.05}\text{Mn}_{0.05}\text{Se}$ layer. As a result, the spin-flip processes also weaken and the differently polarized L_4 bands gradually drift apart. The data in Fig. 15 clearly show this.

Let us examine the L_2 band. It is formed by the emission transition inside the semimagnetic layer $\text{Zn}_{0.9}\text{Be}_{0.05}\text{Mn}_{0.05}\text{Se}$ but the presence of the intermediate barrier in the structure and its thickness appreciably changes this band behavior. First of all,

this barrier changes the energy positions of the donor $E_{ZnBeMnSe}^D$ and acceptor $E_{ZnBeMnSe}^A$ levels in the $Zn_{0.9}Be_{0.05}Mn_{0.05}Se$ surface strain layers in zero magnetic field, which form the L_2 band. A sum of $E_{ZnBeMnSe}^D$ and $E_{ZnBeMnSe}^A$ may be determined as the difference between $E_{1H}(0)$ and $E_{L_2}(0T)$. This difference is equal to 31 meV for the $a1$ structure and is larger by approximately 3 meV for the other three structures. Fig. 5 data make it possible to divide a contribution of both $E_{ZnBeMnSe}^D$ and $E_{ZnBeMnSe}^A$ shifts under conversion from the tensed to compressed contact layers of $Zn_{0.9}Be_{0.05}Mn_{0.05}Se$ in formation of the mentioned difference. In the $b1$, $c1$, and $d1$ structures, both L_2^+ and L_1^+ bands intersect in a magnetic field approximately over 1.9 T. In accordance with the rate of both $E_{ZnBeMnSe}^{C+}$ and $E_{ZnBeMnSe}^{V+}$ level shift, it corresponds to $E_{ZnBeMnSe}^D \approx 10$ meV and $E_{ZnBeMnSe}^A \approx 24$ meV. If we compare these values with the same ones for the $a1$ structure¹³, we see that $E_{ZnBeMnSe}^D$ decreases approximately by 5.5 meV and $E_{ZnBeMnSe}^A$ increases approximately by 8.5 meV under conversion from a tension deformation to a compression deformation of the $Zn_{0.9}Be_{0.05}Mn_{0.05}Se$ layers. We explain this in the following way. Under deformation, both spectrum and wave functions of the electrons for the degenerate band are determined by the solution of the wave equation with Hamiltonian having an addition, which determines of the band splitting. This splitting leads to a reconstruction of the impurity spectrum especially if the splitting of the degenerated band grows up to the energy of impurity ionization E_i ²². In our case, it corresponds to an acceptor center case. The case for a donor center is different. A conduction band of $Zn_{0.9}Be_{0.05}Mn_{0.05}Se$ is non-degenerate. For a non-degenerate band, the change of energy of an impurity center $\Delta E_i/E_i$ is only related to the change of the free carrier effective mass and is approximately $\Delta m/m$ ²². For estimation, E_i may be equated to the average value of $E_{ZnBeMnSe}^D$ for the structures with and without the intermediate barrier while ΔE_i may be equated to the deviation from this average value. Then, we conclude that the deformations originated by the lattice mismatches can cause the change of the free electron effective mass²³ by about 20 % in the structures under study.

Another important feature of the L_2 band is its comparative shift relatively to the L_1^+ band if a magnetic field is applied. The L_2^- band does not change its energy position either before or after intersecting with the L_1^+ band position. This means that the spin-up states of impurity electrons do not mix with the spin-down band electron states and form the resonance state in both C and V bands of $Zn_{0.9}Be_{0.05}Mn_{0.05}Se$ in high magnetic fields. The spin-down states of impurity electrons mix with the spin-down band electron states in high magnetic fields. Therefore, the energy of the L_2^+ band decreases if the $E_{ZnBeMnSe}^A$ level intersects the $E_{ZnBeMnSe}^{V+}$ edge (the $a1$ structure, Fig. 5) or the band disappears if both $E_{ZnBeMnSe}^A$ and $E_{ZnBeMnSe}^D$ levels intersect $E_{ZnBeMnSe}^{V+}$

and $E_{ZnBeMnSe}^{C+}$ edges, respectively (both $b1$ and $c1$ structure, Fig 5). It is not entirely clear why the resonance spin-down states of impurity electrons appear in the C and V band of strained $Zn_{0.9}Be_{0.05}Mn_{0.05}Se$ layers in the $d1$ structure with the thickest intermediate barrier in high magnetic field as well as why the spin-up states of impurity electrons disappear in both $a1$ and $b1$ structures in relatively low magnetic fields.

Let us now examine some aspects of the PL intensity related to the presence of the $Zn_{0.943}Be_{0.057}Se$ intermediate barrier in the structures under study and its effect on the transfer of magnetic interaction between the semimagnetic $Zn_{0.9}Be_{0.05}Mn_{0.05}Se$ layer and non-magnetic $ZnSe$ QW. The first one is the barrier effect on the intensity of the 2D excitons of the $ZnSe$ QW in zero magnetic fields. As one can see in Fig. 8, this intensity increases if the intermediate barrier is applied and $d(Zn_{0.943}Be_{0.057}Se)$ increases. We explain this in the following way. Applying the intermediate barrier we equalize the strain on the both sides of the QW. The strain equalization becomes more effective when the intermediate barrier thickness increases. A decrease of the structure inhomogeneity naturally leads to an increase of emitting recombination.

The second aspect is the barrier effect on the field dependence of the intensity of L_4 bands in low magnetic fields. Giant Zeeman splitting of the band edges of the $Zn_{0.9}Be_{0.05}Mn_{0.05}Se$ layer is an immediate cause of this effect. Applying a magnetic field we decrease both $E_{ZnBeMnSe}^{C+}$ and $E_{ZnBeMnSe}^{V+}$ edges of the C and V bands of the $Zn_{0.9}Be_{0.05}Mn_{0.05}Se$ layer. As a result, the $Zn_{0.943}Be_{0.057}Se$ barrier confines the thermalized carriers in this layer and counteracts their transfer into the $ZnSe$ QW layer. The larger is magnetic field, the stronger is the carrier confinement in the $Zn_{0.9}Be_{0.05}Mn_{0.05}Se$ layer. Since the PL intensity is lower if a concentration of the recombining electrons and holes is smaller, both $I(L_{4(1)}^+)$ and $I(L_{4(2)}^+)$ decrease if B increases.

A recombining carrier concentration is not only a factor defined PL intensity. It especially depends on the emission probability, which, for its part, is proportional to a density of states of the free carriers²⁴. A magnetic field applied transversely to the structure layers transforms the free 2D carriers in the $ZnSe$ QW to 0D carrier if B increases to the quantum strong limit. In this field range a density of states of the carrier is defined by B and increases if B increases. Therefore, the intensity of L_4^+ bands has to change a decrease for an increase if a magnetic field passes in the range of quantum magnetic fields. As one can see from Fig. 9 (right), $I(L_4^+)$ starts increasing at $B > 0.75$ T. Using $m_{hh} = 0.6 m_o$ ²⁵, for this B value we obtain a hole cyclotron energy $\hbar\omega_c \approx 0.14$ meV. The thermal energy of the experiment is $k_oT \approx 0.1$ meV. Therefore, for $B > 0.75$ T, the condition of quantum magnetic fields is already in progress. As a result, two factors determine the further behavior of $I(L_4^+)$ in a magnetic field: a confinement of the free carrier in the

$Zn_{0.9}Be_{0.05}Mn_{0.05}Se$ layer by the $Zn_{0.943}Be_{0.057}Se$ barrier and an increase of the state density of the 0D carriers in the $ZnSe$ QW if B increases. The latter factor dominates and $I(L_4^+)$ increases.

IX. CONCLUSIONS

In this paper we have reported the measurements of luminescence of the 150 nm $Zn_{0.9}Be_{0.05}Mn_{0.05}Se$ / d nm $Zn_{0.943}Be_{0.057}Se$ / 2.5 nm $ZnSe$ / 30 nm $Zn_{0.943}Be_{0.057}Se$ structures as a function of thickness d of the intermediate nonmagnetic barrier $Zn_{0.943}Be_{0.057}Se$ between the $Zn_{0.9}Be_{0.05}Mn_{0.05}Se$ semimagnetic barrier and $ZnSe$ QW and magnetic field at the low temperature 1.2 K. Strong evidence has been obtained that the intermediate nonmagnetic barrier: (i) changes the energy of the PL bands in both the $ZnSe$ QW and $Zn_{0.9}Be_{0.05}Mn_{0.05}Se$ semimagnetic barrier layers; (ii) increases the total PL intensity of the structures; (iii) decreases the degree of circular polarization of the QW exciton emission in the structure; (iv) extinguishes the PL band caused by the indirect transitions in real space between the 2D conduction band of the $ZnSe$ QW and both the Mn complex and the valence band of the $Zn_{0.9}Be_{0.05}Mn_{0.05}Se$ layer. The obtained data enable us to conclude that the emission bands appearing in the semimagnetic $Zn_{0.9}Be_{0.05}Mn_{0.05}Se$ barrier of the structures under study are formed in the contact layers strained by the intermediate $Zn_{0.943}Be_{0.057}Se$ or $ZnSe$ layers. The shifts of the band gap as well as of the donor and acceptor levels under the effect of biaxial compression of the $Zn_{0.9}Be_{0.05}Mn_{0.05}Se$ layer by the $Zn_{0.943}Be_{0.057}Se$ layer are estimated.

It is revealed that there are two different rates $(\chi N_0)_{1H}$

and $(\chi N_0)_{1L}$ of the shift of the short wave bands of the PL spectra of the structure under study in a magnetic field caused by giant Zeeman splitting. The larger rate $(\chi N_0)_{1H}$ is observed in the high magnetic fields and corresponds to the emission transition between C and V bands of the $Zn_{0.9}Be_{0.05}Mn_{0.05}Se$ barrier. A smaller rate $(\chi N_0)_{1L}$ is observed in low magnetic fields and corresponds to the emission transition between the $Zn_{0.9}Be_{0.05}Mn_{0.05}Se$ conduction band and an energy level of the acceptor complex containing Mn . The intermediate nonmagnetic barrier $Zn_{0.943}Be_{0.057}Se$ does not change the $(\chi N_0)_{1H}$ value and accordingly its constituents αN_0 and βN_0 values, which are equal to $\alpha N_0 = 0.104$ eV and $\beta N_0 = -0.264$ eV. At the same time, it decreases the $(\chi N_0)_{1L}$ value by approximately 22 % which we interpret as a decrease of the exchange integral for electronic states of the Mn complex in the $Zn_{0.9}Be_{0.05}Mn_{0.05}Se$ barrier by approximately 40 % (from 0.156 to 0.112 eV) under the effect of the intermediate $Zn_{0.943}Be_{0.057}Se$ barrier. This supports the assumption that: (i) the deformation of the $Zn_{0.9}Be_{0.05}Mn_{0.05}Se$ layers plays a key role in forming the Mn complexes; (ii) the 2D carriers of the $ZnSe$ QW provide a substantial contribution to the formation of the exchange integral for the Mn complexes in strained layers. The $Zn_{0.943}Be_{0.057}Se$ intermediate barrier changes the effect of giant Zeeman splitting of the semimagnetic $Zn_{0.9}Be_{0.05}Mn_{0.05}Se$ barrier energy levels on a move of the energy levels of $ZnSe$ QW in a magnetic field and a polarization of the QW exciton emission.

ACKNOWLEDGMENTS

AS would like to thank the Concept for the Future in the Excellence Initiative at KIT for financial support.

* Taras.Slobodskyy@iss.fzk.de

¹ J.K. Furdyna, J. Appl. Phys. **64**, R29 - R64 (1988)

² Semiconductor Spintronics and Quantum Computation, edited by D.D. Awschalom, D. Loss, and N. Samarth (Springer-Verlag, Berlin, 2002).

³ Spin Physics in Semiconductors, edited by M.I. Dyakonov (Springer-Verlag, Berlin, 2008)

⁴ B.T. Jonker, Y.D. Park, B.R. Bennett, H.D. Cheong, G. Kioseoglou, A. Petrou, Phys. Rev. B **62**, 8180 (2000).

⁵ C. Gould, A. Slobodskyy, T. Slobodskyy, P. Grabs, C.R. Becker, G. Schmidt, and L.W. Molenkamp, physica status solidi (b) **241**, 700 (2004).

⁶ A.A. Maksimov, D.R. Yakovlev, J. Debus, I.I. Tartakovskii, A. Waag, G. Karczewski, T. Wojtowicz, J. Kosut, and M. Bayer, Phys. Rev. B **82**, 035211 (2010).

⁷ M. Kim, C.S. Kim, S. Lee, J.K. Furdyna, and M. Dobrowolska, J. Cryst. Growth, **214/215**, 325-329 (2000).

⁸ A. Slobodskyy, C. Gould, T. Slobodskyy, C.R. Becker, G. Schmidt, and L.W. Molenkamp, Phys. Rev. Lett. **90**, 246601 (2003).

⁹ M.K. Kneip, D.R. Yakovlev, M. Bayer, T. Slobodskyy, G. Schmidt, and L.W. Molenkamp, Appl. Phys. Lett. **88**, 212105 (2006).

¹⁰ G. V. Astakhov, R. I. Dzhiyev, K. V. Kavokin, V. L. Korenev, M. V. Lazarev, M. N. Tkachuk, Yu. G. Kusrayev, T. Kiessling, W. Ossau, and L. W. Molenkamp, Phys. Rev. Lett. **101**, 076602 (2008).

¹¹ G. V. Astakhov, M. M. Glazov, D. R. Yakovlev, E. A. Zhukov, W. Ossau, L. W. Molenkamp, and M. Bayer, Semicond. Sci. Technol. **23**, 114001 (2008).

¹² M.I. Dyakonov and V.I. Perel, "Optical orientation in a system of electrons and lattice nuclei in semiconductors. Theory", Sov. Phys. JETP **38**, 177 (1974).

¹³ D.M. Zayachuk, T. Slobodskyy, G. Astakhov, C. Gould, G. Schmidt, W. Ossau, and L.W. Molenkamp, EPL **91**, 67007 (2010).

¹⁴ D. Keller, D.R. Yakovlev, B. König, W. Ossau, Th. Gruber, A. Waag, L.W. Molenkamp, and A.V. Scherbakov, Phys. Rev. B **65**, 035313 (2001).

- ¹⁵ H. Hoffmann, G. V. Astakhov, T. Kiessling, W. Ossau, G. Karczewski, T. Wojtowicz, J. Kossut, and L. W. Molenkamp, *Phys. Rev. B* **74**, 073407 (2006).
- ¹⁶ N. Dai, L.R. Ram-Mohan, H. Luo, G.L. Yang, F.C. Zhang, M. Dobrowolska, and J.K. Furdyna, *Phys. Rev. B* **50**, 18153 (1994).
- ¹⁷ B. Rockwell, H. R. Chandrasekhar, M. Chandrasekhar, A. K. Ramdas, M. Kobayashi, and R. L. Gunshor, *Phys. Rev. B* **44**, 11307 (1991).
- ¹⁸ W. Faschinger, M. Ehinger, T. Schallenberg, M. Korn, *Appl. Phys. Lett.* **74**, 3404 (1999).
- ¹⁹ A.R. Denton and N.W. Ashcroft, *Phys. Rev. A* **43**, 3161 (1991).
- ²⁰ X.-C. Zhang, S.-K. Chang, A.V. Nurmikko, L.A. Kolodziejski, R.L. Gunshor, and S. Datta, *Phys. Rev. B* **31**, 4056 (1985).
- ²¹ Landolt-Börnstein. II-VI and I-VI Compounds; Semimagnetic Compounds, volume III, chapter 41b. (Springer, Berlin, 1999).
- ²² G.L. Bir and G.E. Picus, *Symmetry and Deformation in Semiconductors* (Science, Moscow, 1972) (in Russian).
- ²³ Charles Kittel *Introduction to Solid State Physics* (7th Edition ed.) (Wiley, New York, 1996).
- ²⁴ Peter Y. Yu Manuel Cardona, *Fundamentals of Semiconductor* (Springer, Berlin, 2005).
- ²⁵ H.J. Lozykowski, V.K. Shastri, *J. Appl. Phys.* **69**, 3235 (1991).